




Remote estimation of leaf water concentration in winter wheat under different nitrogen treatments and plant growth stages

Li He^{1,2,3} · Meng-Ran Liu¹ · Shao-Hua Zhang¹ · Han-Wen Guan¹ · Chen-Yang Wang^{1,3} · Wei Feng^{1,2,3}  · Tian-Cai Guo^{1,3}

Accepted: 14 December 2022 / Published online: 23 December 2022

© The Author(s), under exclusive licence to Springer Science+Business Media, LLC, part of Springer Nature 2022

Abstract

Hyperspectral remote sensing can quickly, nondestructively and accurately monitor crop water concentration and provide technical support for winter wheat growth monitoring, drought assessment, and variable irrigation. In this study, canopy spectral reflectance, leaf water concentration (LWC), leaf nitrogen concentration (LNC), leaf area index (LAI), and leaf dry matter (LDM) of four wheat cultivars were measured under different irrigation and nitrogen treatments, and the effects of nitrogen treatment and growth period on spectral reflectance and LWC were analyzed. Canopy spectral reflectance for different growth periods, irrigation, and nitrogen treatments showed significant changes, leading to the phenomena of “nitrogen treatment differentiation” and “growth period differentiation” for the normalized difference spectral index [NDSI (762, 1458, 2301)] and normalized difference infrared index (NDII) monitoring models. To reduce the influence of nitrogen treatment and growth period on the LWC estimation model, a modified normalized difference water index (mNDWI) was constructed by introducing the nitrogen factor (ratio of left and right peak area, RIDA) into the optimized combination of water-sensitive bands [ND (815, 1080), ND (1585, 1740), and ND (2030, 2260)]. Compared with NDSI (762, 1458, 2301), the R^2 of mNDWI was improved by 36.2%–41.1% under different nitrogen levels and 18.6%–22.4% in different growth periods; this effectively reduced the impact of nitrogen status on LWC monitoring and realized the unified modeling and accurate inversion of LWC for the entire growth period. The new index mNDWI, especially mNDWI (815, 1080) and mNDWI (2030, 2260), can effectively monitor the LWC status of wheat under different cultivation conditions, which is important for the real-time diagnosis of plant moisture to guide precision field irrigation applications.

Keywords Leaf water concentration · Nitrogen treatment · Growth period · Winter wheat · Hyperspectral monitoring

✉ Wei Feng
fengwei78@126.com

✉ Tian-Cai Guo
gtcwheat@henau.edu.cn

Extended author information available on the last page of the article

Introduction

Water is an indispensable and important condition in the process of crop growth. Leaf water concentration (LWC) is a diagnostic variable used to measure crop seedling health and drought. With global warming, droughts tend to occur frequently and seriously (Wang et al., 2015), which aggravates the contradiction between “water decreasing” and “grain increasing” in the Huang Huai Hai Plain. Therefore, real-time accurate monitoring and diagnosis of crop water status is conducive to timely water management and efficient use of water resources to obtain higher yield and better quality in agricultural production. This has important theoretical and practical significance for guiding water-saving agricultural production, and is also one of the most important research topics in modern precision agriculture.

Vegetation color, water content, morphological structure, and physiological composition often change with the amount of irrigation, which in turn causes changes in spectral reflectance characteristics (Gizaw et al., 2016). Leaf reflectance in the 1450–1930 nm band is significantly correlated with LWC in cotton (Thomas et al., 1971). The first derivative of the water absorption band (1360–1470 nm and 1830–2080 nm) is highly correlated with LWC and was not affected by the leaf structure (Danson et al., 1992). The absorption peak in the range of 950–970 nm can be used to monitor plant water content in gerbera, pepper, and bean (Peñuelas et al., 1993). The characteristic wavelength of 522–2450 nm reflectance and its spectral reflectance ratios at 1430, 1650, 1850, 1920 and 1950 nm can be used to estimate multiple water variables of herbaceous and woody plants (Yu et al., 2000). The sensitive band of leaf equivalent water thickness (EWT) is concentrated in the short-wave infrared (SWIR) range, 1400–2500 nm. Since the SWIR reflectance is also affected by the leaf internal structure and biomass, it is not possible to monitor the leaf EWT only by using the SWIR (Ceccato et al., 2001). The sensitive bands of leaf water potential, relative water content, and leaf EWT for spring wheat are concentrated in the visible band (351, 518 and 687 nm), near infrared (NIR; 762, 974, 1100 and 1240 nm), and SWIR (1392, 1515, 1930 and 2273 nm) (Hendawy et al., 2019). Interestingly, similar bands, such as 910, 1020, 1510, and 2300 nm, are related to the absorption of protein and nitrogen, especially for the strong O–H bond at 1940 nm, which is not only associated with N, but also related to water absorption, lignin, and cellulose (Berger et al., 2020).

The vegetation index and derivative spectra constructed by using water-sensitive bands can effectively overcome the shortcomings of low single-band spectrum prediction accuracy. The normalized difference water index (NDWI) was constructed to monitor the vegetation canopy water status (Gao, 1996). The water index, WI (R900/R970), can be used to monitor the water status of forests and shrubs (Peñuelas et al., 1997). The ratio index WI/NDVI can effectively reduce the influence of leaf shape on the estimation of LWC (Peñuelas & Inoue, 1999). Many researchers have further revised and explored new indices on the basis of WI. Strachan et al. (2002) found that the water spectrum absorption peak was shifted, and proposed that the fWBI is defined by the ratio of R900 and the minimum value between R930 and R980, which further revised the WI and improved the monitoring accuracy of water status. Ratio-type vegetation indices (VIs) were constructed to estimate vegetation water status. The simple ratio water index (SRWI) can effectively indicate the leaf EWT for high LAI values (Zarco-Tejada et al., 2003). DR1647/DR1133 and DR1653/DR1687 were the best estimation indices for leaf EWT and fuel moisture content in cotton, respectively (Yi et al., 2013). Das et al. (2017) analyzed the correlation between the spectral data of 10 different wheat varieties and the relative water content, and found that

the best spectral indices are RSI (1391, 1830) and NDSI (1391, 1830). In addition, normalized-type VIs are also suitable for monitoring plant water concentration. MODIS NIR and SWIR bands were used to construct normalized difference water indices ($NDWI_{858, 2130}$) for monitoring the vegetation water content of corn and soybeans (Chen et al., 2005). The normalized multi-band drought index (NMDI) was constructed to monitor canopy moisture (Wang & Qu, 2007). The normalized difference infrared index (NDII) can effectively monitor leaf EWT, which indirectly indicates the water content of corn and soybeans (Yilmaz et al., 2008). The normalized water index ($NWI_{970, 900}$ and $NWI_{970, 920}$) had a better prediction effect on wheat water content (Bandyopadhyay et al., 2014). Yao et al. (2014) introduced the third band in NDSI (1429, 416), which weakened the influence of LNC on monitoring the leaf EWT of wheat. These classic vegetation index modeling methods have the characteristics of fewer input variables and large-scale mapping, which can then guide water irrigation management on a large scale to further improve the water utilization rate.

Previous studies have also made good progress in different methods and different crops for water monitoring (Das et al., 2017; Zhao et al., 2013b). With the development of artificial intelligence, more advanced and adaptive machine learning methods are gaining traction and recognition. The combination of PLSR and vegetation index can further improve the water content estimation in wheat (Elsayed et al., 2017). PLSR followed by multiple linear regression (MLR), artificial neural networks (ANN), support vector machine (SVM), and random forest (RF) models could be used calculate relative water content (RWC) in rice (Krishna et al., 2019). Machine learning relies heavily on the selection of training data, and requires massive data sets to train on. This approach is highly susceptible to errors when a training set is not representative of diverse field experimental conditions or environmental states. Physical-based model inversion methods are considered to be a promising alternative to accurately retrieve biochemical and biophysical vegetation variables. Based on the Beer–Lambert law, the EWT_{leaf} and EWT_{ear} of wheat can be successfully determined (Wocher et al., 2018). The wavelet features derived from PROSPECT simulations can be used to assess predictive models of gravimetric water content (GWC) (Cheng et al., 2012). Although radiative transfer model (RTM)-based inversion methods are considered physically sound, it is challenging to apply them to remote sensing observations because plant biophysical and biochemical properties greatly affect light penetration and scattering. This leads to significant bias for simulating directional reflectance, and different parameter sets may simulate the same reflectance spectrum.

Water and nitrogen are the most important nutrient elements for crops, and they have mutual influences on crop growth, which directly affects crop morphological development and growth status. Studies have shown that under normal irrigation conditions, there is a positive interaction between the nitrogen concentration and the amount of water provided (Klem et al., 2018). Proper application of fertilizer can promote root growth that ensures water uptake from the soil (Cooper et al., 1987). In contrast, nitrogen stress generally reduces crop water conductivity, leading to a decreased LWC (Quintero et al., 1999). Water increases the availability of nutrients, and nutrients also increase water use efficiency, thereby promoting the full utilization of water and fertilizer resources by crops (Wang et al., 2014). Actual field production often involves different levels of nitrogen nutrition, and these will also affect the crop water concentration and other biochemical components (such as LNC) and morphological structures [i.e., LAI and leaf dry matter (LDM)], thus affecting the leaf or canopy spectral reflectance (Berger et al., 2020). Therefore, crop water monitoring must comprehensively consider the leaf and canopy spectral reflectance effects of different nitrogen levels on crop water status. Growth stage is an important influencing factor on the estimation of LWC; crop canopy structure and the background information

of winter wheat will change with plant growth period. Wang et al. (2011) showed that λ_{\min} was a good indicator for monitoring LWC at the booting and milking stages when the soil exposure was relatively large. The monitoring model performed differently before and after anthesis, because nutrients are transported from the leaves to the grains, which affects the physiological and biochemical changes in the organizational structures of leaves (Yao et al., 2014). Kong et al. (2021) analyzed the relationships between spectral indices and LWC of wheat based on the heading and milk-filling periods. The sensitivity differences of the vegetation index to LWC for the different growth period conditions made it difficult to construct a unified LWC monitoring model covering the entire growth period.

The above studies have shown that it is feasible to use spectral monitoring technology to perform non-destructive estimation of LWC; however, these studies seldom consider the coupling of water and nitrogen in the field, and the uncoupling effect of sensitive bands around water and nitrogen. What is needed are not only rapid and easily implemented methods, but also the ability to map large-scale farmland irrigation conditions in agricultural production. In view of this, the quantitative relationships between the LWC and canopy spectra of winter wheat at four nitrogen application levels under different growth periods were analyzed, a new spectral index that weakens the influence of nitrogen and growth periods was explored, and a high-precision winter wheat LWC hyperspectral monitoring model was established. The results of this study will help further understanding of the spectral mechanisms of water and nitrogen interactions, and provide technical support for the rapid monitoring of winter wheat water status under different irrigation treatments and field precision irrigation using unmanned aerial vehicles (UAVs) in the future.

Materials and methods

Experimental design

Experiment 1 was conducted at the experimental station of Henan Agricultural University in Yuanyang County (35°6'N, 114°37'E), Xinxiang City from 2016 to 2017. The tested wheat cultivar was 'Zhoumai 27', the previous crop was corn, and the corn straw was crushed and returned to the field after harvest. The pH of the soil layer at 0–200 mm before planting was 7.8, and it contained 13.2 g kg⁻¹ of organic matter, 0.81 g kg⁻¹ of total nitrogen, 13.6 mg kg⁻¹ of available phosphorus, and 156.2 mg kg⁻¹ of available potassium. The total precipitation was 194 mm from sowing to harvest. The experiment was a random split zone design. The main zone had three irrigation frequencies; W0 (no added water), W1 (watered once at the jointing stage), and W2 (watered once at the jointing stage and once at anthesis). The irrigation volume was 750 m³ ha⁻¹ both times, and soil water concentration was kept at 75%–80% by the traditional gravimetric method. The subplot stratum was randomly assigned five nitrogen levels: 0 (N0), 90 (N1), 180 (N2), 270 (N3), and 360 (N4) kg ha⁻¹ pure nitrogen (as urea), 50% of which was base fertilizer applied before sowing and 50% was top dressing applied at jointing. 150 kg ha⁻¹ P₂O₅ (as monocalcium phosphate [Ca(H₂PO₄)₂]) and 90 kg ha⁻¹ K₂O (as KCl) were applied prior to seeding for all treatments. The experimental plot was 39 m², the row spacing was 200 mm, the basic seedling density was 360 × 10⁴ plants ha⁻¹, and there were three replicates. Spectroscopic measurements and sampling were performed from the regreening stage to the late grain filling stage, and the yield was measured at maturity.

Experiment 2 was conducted at Luoyang Academy of Agricultural Sciences in Henan Province (34°38'N, 112°29'E) from 2017 to 2018. Wheat cultivars 'Luohan 22', 'Zhongmai 175', 'Zhoumai 27', and 'Jinmai 47', which have different levels of drought tolerance, were selected as the test cultivars. The first crop was corn, and the straw was returned to the field after harvest. The pH of the soil layer at 0–200 mm before planting was 8.0, and it contained 26.1 g kg⁻¹ of organic matter, 0.15 g kg⁻¹ of total nitrogen, 52.7 mg kg⁻¹ of available phosphorus, and 56.7 mg kg⁻¹ of available potassium. The precipitation was 339.4 mm from sowing to harvest. The experiment was a random block design, and the main area had four irrigation frequencies; W0 (dry shed treatment, no irrigation during the whole growth period), W1 (natural precipitation), W2 (watering once at the jointing stage), and W3 (watering once at the jointing stage and again in the early grain filling stage). The irrigation volume was 750 m³ ha⁻¹ for the jointing stage and 600 m³ ha⁻¹ for the early grain filling stage because the precipitation was 103.6 mm in May. The subplot was the variety treatment, and the experiment was repeated three times. The level of nitrogen (as urea) applied to all test plots was the same (270 kg ha⁻¹), of which 50% was base fertilizer applied before sowing and 50% was top dressing applied at jointing. 150 kg ha⁻¹ P₂O₅ (as monocalcium phosphate [Ca(H₂PO₄)₂]) and 90 kg ha⁻¹ K₂O (as KCl) were applied prior to seeding for all treatments. The experimental plots were 2 m² and the row spacing was 250 mm. Spectroscopic measurements and sampling were performed from the regreening stage to the late grain filling stage, and the yield was measured at maturity.

Experiment 3 was conducted at the experimental station of Henan Agricultural University in Yuanyang County (35°6'N, 114°37'E), Xinxiang City from 2018 to 2019. The tested wheat cultivars were 'Yumai 49-198', 'Fengdechunmai 5', and 'Zhengmai 103'. The previous crop was corn, and the corn straw was crushed and returned to the field after harvest. The pH of the soil layer at 0–200 mm before planting was 7.9, and it contained 14.3 g kg⁻¹ of organic matter, 0.82 g kg⁻¹ of total nitrogen, 12.8 mg kg⁻¹ of available phosphorus, and 144.2 mg kg⁻¹ of available potassium. The total precipitation was 64.3 mm from sowing to harvest. The experiment was a random split zone design, the main zone had two irrigation frequencies; W0 (no added water), and W1 (watered once at the jointing stage, irrigation volume was 750 m³ ha⁻¹), and the subplot stratum was randomly assigned five nitrogen levels: 0 (N0), 90 (N1), 180 (N2), 270 (N3), and 360 (N4) kg ha⁻¹ pure nitrogen (as urea), 50% of which was base fertilizer applied before sowing and 50% was applied as topdressing at jointing. 150 kg ha⁻¹ P₂O₅ (as monocalcium phosphate [Ca(H₂PO₄)₂]) and 90 kg ha⁻¹ K₂O (as KCl) were applied prior to seeding for all treatments. The experimental plot was 39 m², the row spacing was 200 mm, the basic seedling density was 360 × 10⁴ plants ha⁻¹, and there were three replicates. Spectroscopic measurements and sampling were performed from the jointing stage to the late grain filling stage, and the yield was measured at maturity (Table 1).

Measurement of canopy spectral reflectance

A back-mounted field spectroradiometer (Field Spec FR Pro2500, Analytical Spectral Devices, Boulder, CO, USA) with a 25° field-of-view fiber optic adaptor was used to measure the canopy spectral reflectance of the winter wheat. Reflectance was calculated as the ratio between the energy reflected by the canopy and the energy incident upon the canopy (i.e., canopy reflectance is a relative measure, with values that range from 0 to 1). The instrument's waveband range was 350–2500 nm, sampling interval was 1.4 nm, spectral resolution was 3 nm in the 350–1000 nm spectral range, sampling interval was 1.1 nm, and

Table 1 Growing seasons, soil characteristics, wheat cultivars, water and nitrogen treatments, and sampling dates for the three field experiments

Exp No	Season and site	Soil characteristics and total precipitation	Cultivar	Water treatment	N treatment (kg hm ⁻²)	Sampling stage
Exp.1	2016–2017 Yuanyang County	Type: fluvo-aquic soil, Organic-M: 13.2 g kg ⁻¹ , Soil pH (CaCl ₂): 7.8, Total N: 0.81 g kg ⁻¹ , Available P: 13.6 mg kg ⁻¹ , Available K: 156.2 mg kg ⁻¹ Precipitation: 194.0 mm	‘Zhoumai 27’	W0 (no water added), W1 (watered once at the jointing stage), W2 (watered once at the jointing stage and once again at the flowering stage)	0 (N0), 90 (N1), 180 (N2), 270 (N3), 360 (N4)	Regreening, Jointing, Booting, Anthesis, Early-filling, Mid-filling, Late-filling
Exp.2	2017–2018 Luoyang City	Type: fluvo-aquic soil, Organic-M: 26.1 g kg ⁻¹ , Soil pH (CaCl ₂): 8.0, Total N: 0.15 g kg ⁻¹ , Available P: 52.7 mg kg ⁻¹ , Available K: 56.7 mg kg ⁻¹ Precipitation: 339.4 mm	‘Luohan 22’, ‘Zhongmai 175’, ‘Zhoumai 27’, ‘Jinmai 47’	W0 (no irrigation during the entire growth period), W1 (natural precipitation), W2 (watered once at the jointing stage), W3 (watered once at the jointing stage and once again in the early stage of filling)	270 (N3)	Regreening, Jointing, Booting, Anthesis, Early-filling, Mid-filling, Late-filling
Exp.3	2018–2019 Yuanyang County	Type: fluvo-aquic soil, Organic-M: 14.3 g kg ⁻¹ , Soil pH (CaCl ₂): 7.9, Total N: 0.82 g kg ⁻¹ , Available P: 12.8 mg kg ⁻¹ , Available K: 144.2 mg kg ⁻¹ Precipitation: 64.3 mm	‘Yumai 49–198’, ‘Fengdehummai 5’, ‘Zhengmai 103’	W0 (no irrigation during the entire growth period), W1 (watered once at the jointing stage),	0 (N0), 90 (N1), 180 (N2), 270 (N3), 360 (N4)	Jointing, Booting, Anthesis, Early-filling, Mid-filling

the spectral resolution was 10 nm in the 1001–2500 nm spectral range. Spectrum acquisition was synchronized with the agronomic sampling times, at the regreening stage, jointing stage, booting stage, anthesis, early filling stage, middle filling stage, and late filling stage of the winter wheat. The winter wheat canopy spectral reflectance was measured at 10:00–14:00 during sunny and windless weather. The spectrometer probe was oriented vertically downward, 1 m above the canopy's top by skilled manual fixation. In order to obtain a more representative canopy reflectance, three sampling points were selected in each plot, five spectra were collected at each location, and these 15 spectra were averaged as the spectrum samples for the entire plot. The noise from the 1350–1500 nm, 1800–1950 nm, and 2475–2500 nm water vapor absorption bands were eliminated. In addition, a standard 0.40 m × 0.40 m whiteboard made of BaSO₄ was used during the measurement process to correct the observation of each group of targets in time.

Determination of agricultural variables

Leaf water concentration and leaf dry matter

Following the spectral measurements, 10 representative plants were selected in each plot and all leaves were quickly removed from the stalks. The leaves were weighed to determine the fresh weight (WF), and then placed in an oven at 105 °C and dried at 80 °C to a constant weight. The dry weight (WD) was then recorded and converted to leaf dry matter (LDM) weight per unit area (t ha⁻¹). The formula for calculating LWC is as follows:

$$\text{LWC}(\%) = (\text{WF} - \text{WD})/\text{WF} \times 100 \quad (1)$$

Leaf nitrogen concentration

Plant samples used for the determination of LNC were dried and crushed separately by tissue/organ type, and their LNC (%) was determined using an automatic Kjeldahl nitrogen analyzer (Kjeltec 2300, FOSS, Sweden) based on the Kjeldahl method.

$$\omega(\text{N}) = c(V_1 - V_0) \times 14 \times V/V_2M \quad (2)$$

where $\omega(\text{N})$ is the mass fraction of leaf total nitrogen (%); c is the acid standard solution (mol. l⁻¹); V_1 is the volume of acid standard liquid used for titrating the sample (ml); V_0 is the acid standard solution (ml) for the titrating blank; 14 was the molar mass of N (g. mol⁻¹); V is the constant volume of dissolving solution (ml); V_2 is the volume measured by suction; M is the leaf sample mass (g).

Leaf area index

The ground-based effective LAI of each experimental plot was measured using a Licor LAI-2000 plant canopy analyzer (LI-COR, Inc., Lincoln, NE, USA).

Selection of vegetation index: For this study, nine vegetation indices related to water for monitoring the wheat LWC were selected. The calculation formulas and sources are shown in Table 2.

Table 2 Calculation methods and references for optimal vegetation indices

Vegetation index	Computational formula	Reference
water index (WI)	$R900/R970$	(Peñuelas et al., 1997)
simple ratio water index (SRWI)	$R860/R1240$	(Zarco-Tejada et al., 2003)
normalized difference water index (NDWI1)	$(R860-R1240)/(R860+R1240)$	(Gao, 1996)
normalized difference infrared index (NDI2)	$(R850-R1650)/(R850+R1650)$	(Yilmaz et al., 2008)
normalized difference water index (NDWI2)	$(R858-R2130)/(R858+R2130)$	(Chen et al., 2005)
shortwave angle normalized index (SANI)	$\text{Angle} (1240) \times (R1640-R858)/(R1640+R858)$	(Orueta et al., 2005)
WI/NDVI (WI/NDVI)	$(R900/R970)/[(R900-R680)/(R900+R680)]$	(Peñuelas & Inoue, 1999)
normalized difference spectral index (NDSI (762,1458,2301))	$(R762-R1458)/(R762+R1458-R2301)$	(Yao et al., 2014)
normalized multi-band drought index (NMDI)	$[R860-(R1640-R2130)]/[R860+(R1640+R2130)]$	(Wang & Qu, 2007)

Construction of a new vegetation index

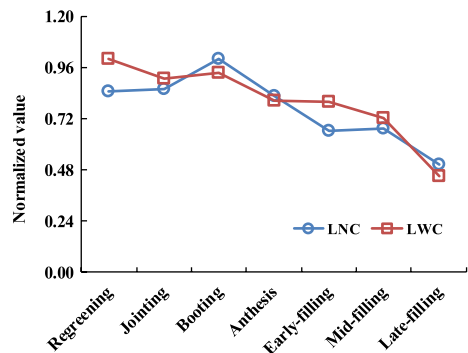
NDVI, the normalized difference vegetation index, is the most widely used vegetation index in remote sensing monitoring research. The sensitive bands of vegetation moisture are mostly located in the bands above the NIR, such as 950 nm, 1240 nm, 1450 nm, 1650 nm, and 2200 nm. On the basis of the water sensitive bands, previous studies have successively established the water vegetation indices NDWI1, NDII, and NDWI2 through the NDVI form of the two-band combination (Chen et al., 2005; Gao, 1996; Yilmaz et al., 2008). Some studies have subsequently improved and optimized it to solve the modeling saturation problem by adding a constant coefficient or new band into the NDVI (Huete et al., 2002; Peng & Gitelson, 2011). Therefore, most vegetation indices can be summarized by a simple framework which corresponds to the modified normalized difference vegetation index (mNDVI).

$$\text{mNDVI} = \frac{(1 + a)R_{\lambda 1} - (1 - a)R_{\lambda 2}}{R_{\lambda 1} + R_{\lambda 2}} \quad (3)$$

where $\lambda 1$ and $\lambda 2$ of the spectral range are located in the wavelength range of 350–2500 nm, $\lambda 1$ is the reference band, and $\lambda 2$ is the sensitive band to the target. “ a ” is a constant coefficient or a new band, “ $1 + a$ ” increases the role of the reference band, and “ $1 - a$ ” reduces the role of the sensitive band.

Plant water concentration and nitrogen concentration are important variables that can be used to characterize crop growth. There is a close relationship between plant water concentration and nitrogen concentration, which is synchronized and synergistic with the plant growth period (Fig. 1). Therefore, it is necessary to reduce the influence of nitrogen concentration when monitoring crop water concentration. The canopy reflectance of green vegetation often exhibits a red-edge bimodal phenomenon due to vegetation type and environment, which is closely related to nitrogen status (Gong et al., 2002; Zarco-Tejada et al., 2001). Some studies used red edge indices as indicators of nitrogen nutrition and plant water content (Cho & Skidmore, 2006; Fitzgerald et al., 2006; Liu et al., 2004). Feng et al. (2014) segmented the red-edge bimodal area and found that the red-edge bimodal parameter was very sensitive to changes in LNC, and the value of the left–right peak area ratio (RIDA) ranged from 0 to 1. This parameter can effectively indicate the nitrogen status of wheat leaves (Fig. 2A), while the sensitivity to LWC was significantly reduced (Fig. 2B).

Fig. 1 Changes in LWC and LNC in wheat across seven different growth stages



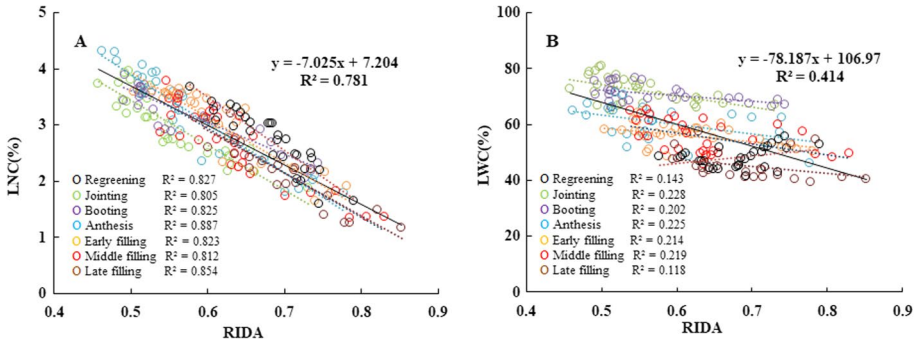


Fig. 2 The relationships of RIDA to LNC (A) and LWC (B) in wheat at seven different growth stages (Color figure online)

$$RIDA = \frac{RSDR}{LSDR} = \int_{718}^{755} \frac{dR\lambda}{d\lambda} d\lambda / \int_{680}^{718} \frac{dR\lambda}{d\lambda} d\lambda \tag{4}$$

RSDR is the sum of the first derivative spectra within the right-side peak of the 718–755 nm region, and LSDR is the sum of the first derivative spectra within the left-side peak of the 680–718 nm region.

For this reason, the left–right peak area ratio (RIDA) was regarded as the influence coefficient (Ne) of the nitrogen factor in the study, and introduced it into the mNDVI. Thus, the formula for the modified water index (mNDWI) is:

$$mNDWI = \frac{(1 + Ne)R_{\lambda 1} - (1 - Ne)R_{\lambda 2}}{R_{\lambda 1} + R_{\lambda 2}} \tag{5}$$

$R_{\lambda 1}$ and $R_{\lambda 2}$ are the canopy spectral reflectances at two different wavebands, $\lambda 1$ is the reference band, and $\lambda 2$ is the sensitive band to water. Ne is the nitrogen factor coefficient; the value is equal to the RIDA, and the range was 0 to 1. “1 + Ne” increases the role of the reference band, and “1 – Ne” attenuates the nitrogen effect of the water sensitive band.

Statistical analysis

The data from Experiments 1 and 2 were used as the calibration set, and the data from Experiment 3 was used as the validation set (Table 3). The spectral data collected in the field was output as spectral reflectance through the software ViewSpec Pro (Analytical Spectral Devices Inc., Colorado, USA), and then the original spectral reflectance was denoised by OriginPro 8.0 (Origin Lab, Inc., USA) using the Savitzky–Golay filter smoothing method. EXCEL2007 and MATLAB 9.0 (MathWorks, Inc., USA) software were used to statistically analyze the LWC and the corresponding spectral reflectance. Ratios, normalized difference and difference vegetation index (RSI, NDSI, DSI) were constructed by the random combination of two bands in the 350–2500 nm range. The accuracy of the model was evaluated by the coefficient of determination (R^2) and the root mean square

Table 3 The dataset range of LWC, LNC, LAI, and LDM used in this study

	Max	Min	Mean	SD	CV (%)	Correlation coefficient (r)
Calibration-LWC	82.47	23.88	60.71	15.28	0.25	
Validate-LWC	83.79	52.71	74.49	6.48	0.09	
Calibration-LAI	8.92	0.40	2.74	1.99	0.73	
Calibration-LDM	3.94	0.10	1.38	0.89	0.64	
LAI vs. LDM						0.89
LAI vs. LNC						0.79
LDM vs. LNC						0.83

error (RMSE). A lower RMSE value indicates that the index has better accuracy in estimating LWC.

$$RSI = \frac{R_{\lambda 1}}{R_{\lambda 2}} \quad (6)$$

$$NDSI = \frac{R_{\lambda 1} - R_{\lambda 2}}{R_{\lambda 1} + R_{\lambda 2}} \quad (7)$$

$$DSI = R_{\lambda 1} - R_{\lambda 2} \quad (8)$$

$$RMSE = \sqrt{\frac{1}{n} \times \sum_{i=1}^n (P_i - O_i)^2} \quad (9)$$

In the formula, P_i is the simulated value of LWC; O_i is the measured value of LWC; n is the number of samples.

Results

Variation in spectral reflectance characteristics of the winter wheat canopy under different water and nitrogen conditions

Different nitrogen and irrigation treatments significantly affected the spectral reflectance of the winter wheat canopy. Figure 3 shows that the change in spectral reflectance at different wavelengths varies with the irrigation treatments (Fig. 3A) and nitrogen levels (Fig. 3B). These results show that the overall trend of changes in the winter wheat canopy spectral characteristics under different water and nitrogen treatments was consistent. With the increase in irrigation frequency and nitrogen level, reflectance of the wheat canopy gradually decreased in the visible waveband (400–700 nm), and increased in the NIR band (780–1350 nm), and there were two obvious absorption valleys in the 970 nm and 1200 nm water characteristic bands; the canopy reflectance

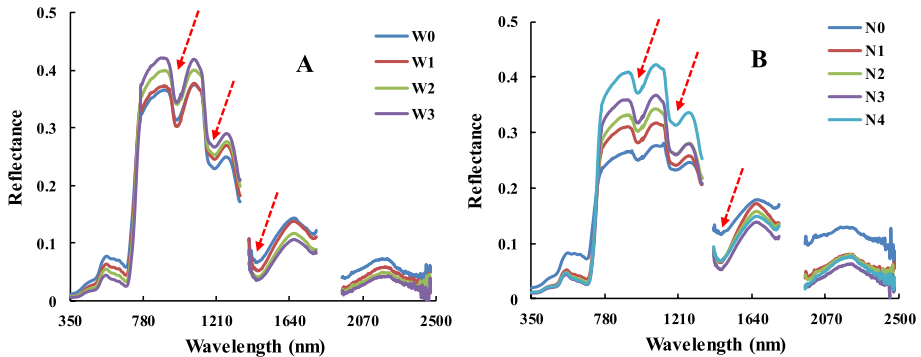


Fig. 3 Spectral reflectance of the wheat canopy for four different water treatments at the N3 level (270 kg ha^{-1}) (A) and for five nitrogen treatments at the W1 level (watered once at the jointing stage) (B) at anthesis

gradually decreased in the SWIR band (1350–2500 nm) with the increases in irrigation times and nitrogen levels, and there were obvious absorption valleys and reflection peaks at 1400 nm and 2200 nm.

The relationship between LWC and vegetation index

The relationships between LWC and nine conventionally-used vegetation indices were tested in different growth periods (Table 4). The monitoring accuracy of the same water vegetation index in different growth periods was different, and the monitoring precision of different water vegetation indices in the same growth period was also different. The correlation between water vegetation index and LWC first increased and then decreased as the growing period advanced. Most of the vegetation indices had the highest correlation with LWC during anthesis and the early grain filling stages ($|R| \geq 0.662$, $\text{RMSE} \leq 8.68\%$), and the lowest correlations occurred during the regreening period ($0.453 \leq |R| \leq 0.682$, $8.30\% \leq \text{RMSE} \leq 14.57\%$). Overall, the correlation between WI and LWC was the worst ($R = 0.597$, $\text{RMSE} = 12.14\%$); NDSI (762, 1458, 2301) and NDII performed better, and the correlations with LWC were 0.827 and 0.795, respectively. However, the phenomenon of “growth period differentiation” appeared when the NDSI (762, 1458, 2301) and NDII were relied upon to monitor LWC during different growth periods, and the monitoring accuracy in the different periods was 0.465–0.724 and 0.394–0.729, and the RMSE was 5.13%–8.30% and 5.95%–8.99% for NDSI and NDII, respectively. Based on the performance under different nitrogen treatments, the overall monitoring effects of NDSI (762, 1458, 2301) and NDII were poor ($R^2 = 0.516$ and 0.454 , $\text{RMSE} = 7.57\%$ and 7.99% for NDSI and NDII, respectively). The monitoring accuracy under each nitrogen treatment showed the phenomenon of “nitrogen treatment differentiation,” and was ≤ 0.681 under high nitrogen (N4) and low nitrogen (N0 and N1) conditions, and was the highest ($R^2 = 0.708$ and 0.760) in the N3 treatment (Fig. 4).

Table 4 The relationships between LWC and common vegetation indices at seven growth stages in winter wheat (n = 434)

Vegetation index		Regreening	Jointing	Booting	Anthesis	Early-filling	Mid-filling	Late-filling	Total
WI	r	0.453	0.632	0.778	0.782	0.788	0.773	0.621	0.597
	RMSE	14.57	9.54	8.85	8.58	8.68	8.84	11.26	12.14
SRWI	r	0.658	0.674	0.781	0.821	0.817	0.801	0.683	0.742
	RMSE	9.85	8.82	8.11	7.48	7.85	8.50	8.96	9.89
NDWI (860,1240)	r	0.572	0.681	0.784	0.816	0.826	0.793	0.676	0.721
	RMSE	9.84	8.65	8.22	7.47	7.76	8.67	8.72	9.92
NDII	r	0.628	0.662	0.732	0.791	0.854	0.787	0.688	0.795
	RMSE	8.99	7.84	7.19	5.95	6.12	7.45	8.51	8.56
NDWI-2	r	0.578	0.658	0.693	0.729	0.812	0.777	0.621	0.715
	RMSE	11.26	9.52	8.10	7.54	7.87	8.45	9.19	10.11
SANI	r	0.678	0.664	0.735	0.794	0.806	0.786	0.709	0.773
	RMSE	9.69	8.60	8.16	7.43	7.81	8.62	8.60	9.35
WI/NDVI	r	-0.607	-0.671	-0.629	-0.684	-0.789	-0.716	-0.686	-0.707
	RMSE	14.36	8.60	8.25	7.51	7.67	8.78	8.97	10.70
NDSI (762,1458,2301)	r	0.682	0.684	0.733	0.821	0.851	0.814	0.725	0.827
	RMSE	8.30	7.49	6.23	5.85	5.13	6.44	8.22	8.18
NMDI	r	0.482	0.558	0.597	0.662	0.689	0.671	0.547	0.662
	RMSE	10.13	10.06	8.31	7.60	7.95	8.47	10.24	11.54

$t_{0.01} = 0.12727$

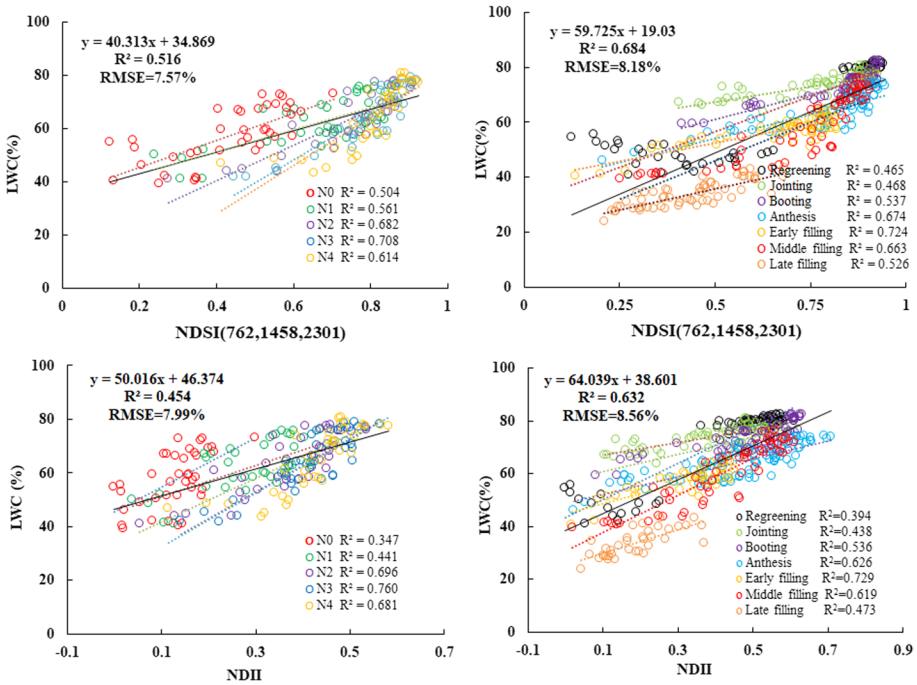


Fig. 4 Quantitative relationships between the LNC and NDSI (762,1458,2301) (left panels) and between the LWC and NDII (right panels) for five different nitrogen treatments and seven growth stages of winter wheat. (nregreening = 73, njointing = 60, nbooting = 76, nflowering = 94, ninitial-filling = 40, nmid-filling = 56, nlate-filling = 36; the number of each N treatment = 39)

Quantitative relationships between two-band vegetation indices and LWC

In order to find the vegetation index that was best related to LWC, the ability of the RSI, NDSI, and DSI of the two-band combinations in the 350–2500 nm range to monitor the LWC were systematically analyzed. The sensitive band regions of RSI and DSI were very small, so the contour maps were not analyzed further. From the two-band normalized contour maps, five sensitive monitoring regions ($R^2 > 0.65$) can be screened

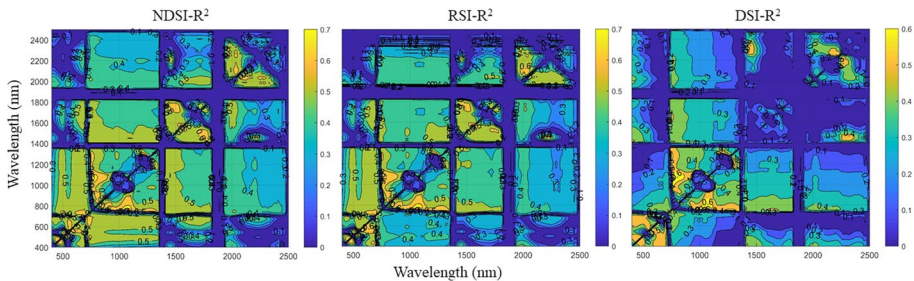


Fig. 5 Contour maps of determination coefficients (R^2) for linear relationships between LWC and NDSI, RSI, and DSI of the possible two-band combinations

out; for the green/red band combination region, the green band was concentrated at 550–560 nm, and the red band was concentrated at 615–630 nm; for the red edge/red band combination region, the red edge band was concentrated at 735–745 nm, and the red band was concentrated at 635–675 nm; for the NIR/NIR band combination region, the NIR bands were concentrated at 770–820 nm and 1020–1120 nm, respectively; for the two SWIR/SWIR band combination regions, the SWIR-1/SWIR-1 bands were concentrated at 1565–1600 nm and 1720–1780 nm, respectively, and the SWIR-2/SWIR-2 bands were concentrated at wavelengths of 2020–2040 nm and 2220–2300 nm, respectively (Fig. 5).

Three large regions (NIR/NIR band combination, SWIR-1/SWIR-1 band combination, and SWIR-2/SWIR-2 band combination) with high monitoring accuracy and wide suitable bands were selected, and the three types of spectral indices with the best correlation in these regions were screened; NDSI (815, 1080) ($R^2=0.729$, RMSE=6.67%), NDSI (1585, 1740) ($R^2=0.657$, RMSE=8.08%), and NDSI (2030, 2260) ($R^2=0.701$, RMSE=7.30%). Compared with the conventional vegetation indices NDII and NDSI (762, 1458, 2301), the ability of these three types of spectral indices to monitor LWC under different nitrogen treatments was improved; this was especially true for the high nitrogen (N4) treatment, in which the monitoring ability was improved the most ($\geq 5.1\%$). Therefore, the accuracy of the overall modeling under different nitrogen treatment conditions was also improved correspondingly, and the improvement rate was $\geq 12.6\%$. Similarly, these three types of vegetation indices weakened the influence of the growth period to a certain extent, which was mainly manifested as a greater increase in the monitoring accuracy of the regreening period and the jointing period ($\geq 28.2\%$) (Fig. 6).

Construction of the mNDWI monitoring model

In order to weaken the influence of nitrogen application levels at different growth periods in the monitoring of winter wheat LWC, RIDA was introduced into three sensitive combination regions (the NIR/NIR band combination, the SWIR-1/SWIR-1 band combination, and the SWIR-2/SWIR-2 band combination). The contour maps of the combined determination coefficients at the three sensitive regions were drawn based on mNDWI (Fig. 7). Compared with two-band normalized contour maps, the sensitive bandwidths of the NIR/NIR band combination, SWIR-1/SWIR-1 band combination, and SWIR-2/SWIR-2 band combination became larger. According to the principle of the largest R^2 for the models, the NIR/NIR band combination is based on central bands of 815 and 1080 nm with bandwidths of 30 nm and 60 nm, respectively. The SWIR-1/SWIR-1 band combination is based on central bands of 1585 and 1740 nm with bandwidths of 80 nm and 40 nm, respectively. The SWIR-2/SWIR-2 band combination is based on central bands of 2030 and 2260 nm with bandwidths of 130 nm and 30 nm, respectively.

The monitoring accuracies of mNDWI (815, 1080), mNDWI (1585, 1740), and mNDWI (2030, 2260) under the different nitrogen treatments were 0.724–0.829, 0.710–0.785, and 0.736–0.831, respectively. Compared with the selected ND (815, 1080), ND (1585, 1740), and ND (2030, 2260), the monitoring accuracy was significantly improved (Table 5). Among them, the relative increase was highest for the N0 treatment (29.8%–33.6%). The R^2 of mNDWI (815, 1080), mNDWI (1585, 1740), and mNDWI (2030, 2260) for the entire nitrogen treatments were 0.716, 0.703, and 0.728, respectively; the RMSEs were 5.53, 6.05, and 5.17%, respectively, and the relative increase was $\geq 12.2\%$. The mNDWI not only greatly alleviated the “differentiation of

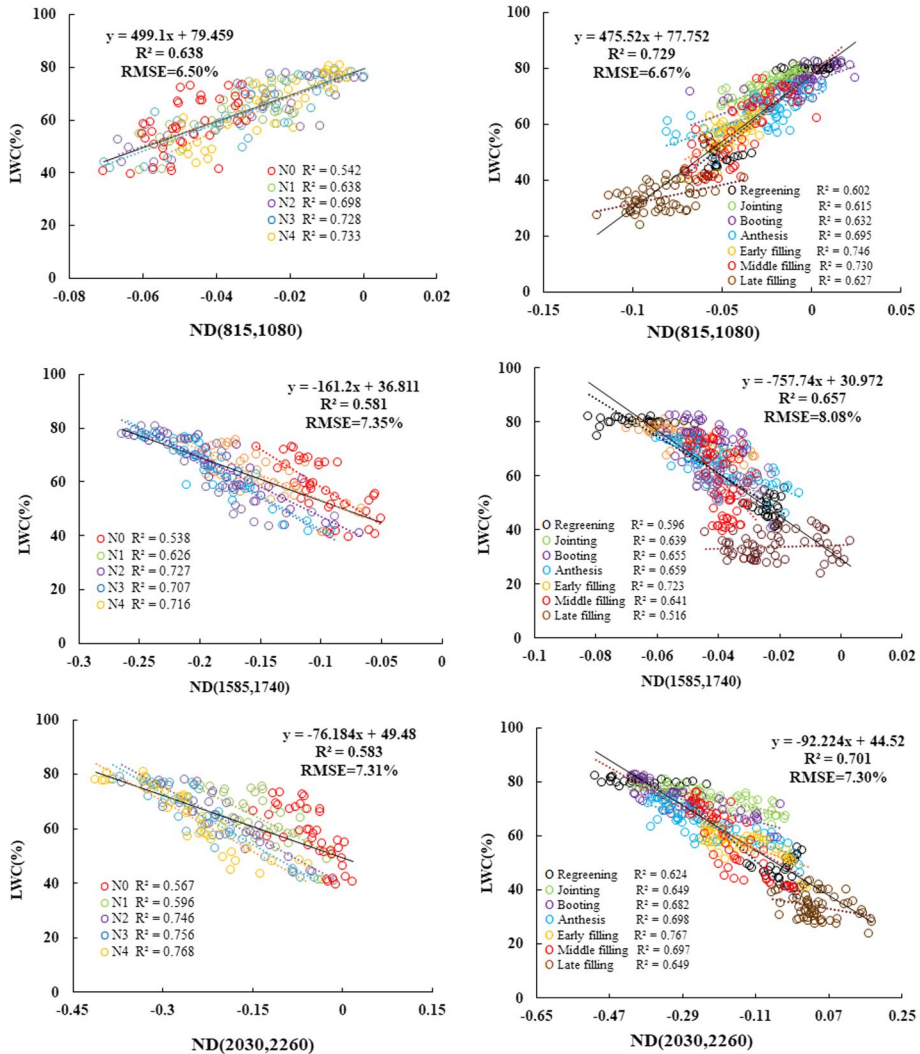


Fig. 6 Quantitative relationships between the LWC and the three optimized two-band combinations NDSI (815, 1080) (left panels), NDSI (1585, 1740) (center panels), and NDSI (2030, 2260) (right panels) for five different nitrogen treatments and seven growth stages. (nregreening=73, njointing=60, nbooting=76, nflowering=94, ninitial-filling=40, nmid-filling=56, nlate-filling=36, the number of each N treatment=39)

nitrogen treatment” phenomenon, but also reduced the effect of the “differentiation of growth period” phenomenon. The monitoring accuracy was improved in each growth period, and it was greatly improved at anthesis and the early grain filling stage, and the relative increases were 16.3%–28.7%. mNDWI (815, 1080), mNDWI (1585, 1740), and mNDWI (2030, 2260) can better monitor the winter wheat LWC throughout the growth period with R^2 values of 0.823, 0.811, and 0.837, respectively, and the RMSEs were 5.64%, 5.92%, and 5.25%, respectively (Fig. 8). The influence of several confounding

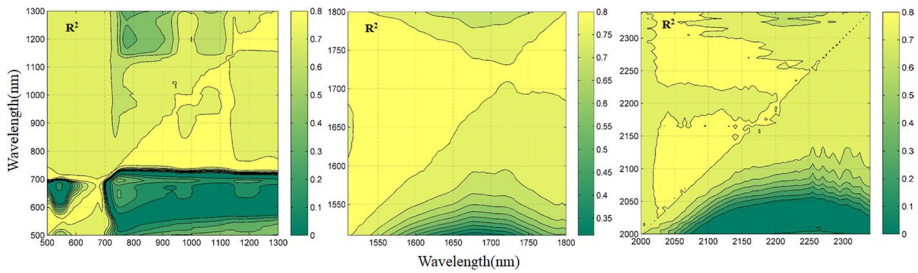


Fig. 7 Contour maps of determination coefficients (R^2) for linear relationships between LWC and the mNDWI of the NIR/NIR band combination (left panel), the SWIR-1/SWIR-1 band combination (center panel), and the SWIR-2/SWIR-2 band combination (right panel)

factors, such as LNC, LAI, and LDM on the mNDWI model were further analyzed. As shown in Fig. 9, the mNDWI (815, 1080), mNDWI (1585, 1740), and mNDWI (2030, 2260) performed poorly, with R^2 values of 0.459, 0.504, and 0.407, and RMSEs of 0.63%, 0.61%, and 0.66% for LNC monitoring; with R^2 values of 0.423, 0.487, and 0.398, and RMSEs of 1.53, 1.49, and 1.56 for LAI monitoring; and R^2 values of 0.408, 0.421, and 0.394, and RMSEs of 0.74 t ha⁻¹, 0.71 t ha⁻¹, and 0.76 t ha⁻¹ for LDM monitoring, respectively.

Testing LWC estimation models

To determine whether the mNDWI (815, 1080), mNDWI (1585, 1740), and mNDWI (2030, 2260) models are reliable for estimating wheat LWC, the three models were tested using an independent dataset obtained from Exp. 3. The 1:1 relationship between the measured and estimated values at five growth periods and five nitrogen application levels helped confirm the reliability and accuracy of the three models. Note that the monitoring model based on mNDWI (1585, 1740) had slightly weaker performance, with R^2 of 0.787 and RMSE 4.78%. The models based on mNDWI (815, 1080) and (2030, 2260) performed better, with R^2 values of 0.803 and 0.820, and RMSEs of 4.51% and 3.58%, respectively (Fig. 10). Therefore, mNDWI, especially mNDWI (815, 1080) and (2030, 2260) could be a good indicator for monitoring LWC in wheat under different nitrogen treatments and at multiple growth stages.

Discussion

The effects of nitrogen on LWC estimation

Water and nitrogen are the main factors that limit plant growth, and they interact in a complex manner. Previous studies have shown that water and nitrogen are indirectly related through chlorophyll and cellulose (Pu et al., 2000). In this study, the changes in the characteristics of LWC and LNC with growth period were systematically analyzed, and found that the trend for both is basically the same and is closely related, indicating that nitrogen may be an important physiological factor affecting crop water monitoring. Taken a step

Table 5 The relationships between two-band indices and mNDWI with LWC at seven growth stages and five nitrogen treatments

	N0	N1	N2	N3	N4	Total	Regreening	Jointing	Booting	Anthesis	Early filling	Middle filling	Late filling	Total
ND (815, 1080)	R ² 0.542	0.638	0.698	0.728	0.733	0.638	0.602	0.615	0.632	0.695	0.746	0.730	0.627	0.729
	RMSE 6.15	4.11	3.34	4.09	5.29	6.50	6.79	5.76	5.52	4.18	4.45	5.16	6.06	6.67
ND (1585, 1740)	R ² 0.538	0.626	0.727	0.707	0.716	0.581	0.596	0.639	0.655	0.659	0.723	0.641	0.516	0.657
	RMSE 7.10	5.82	3.92	4.84	5.83	7.35	8.00	5.90	5.67	4.90	4.82	5.75	6.76	8.08
ND (2030, 2260)	R ² 0.567	0.596	0.746	0.756	0.768	0.583	0.624	0.649	0.682	0.698	0.767	0.697	0.649	0.701
	RMSE 6.34	5.32	3.85	4.54	5.79	7.31	7.15	5.86	5.63	4.45	4.63	5.40	6.33	7.30
mNDWI (815, 1080)	R ² 0.724	0.758	0.829	0.793	0.784	0.716	0.653	0.640	0.794	0.889	0.887	0.801	0.693	0.823
	RMSE 4.85	3.31	3.08	3.80	4.65	5.53	3.81	3.50	3.49	2.49	2.85	3.12	5.10	5.64
mNDWI (1585, 1740)	R ² 0.710	0.752	0.785	0.784	0.738	0.703	0.625	0.633	0.741	0.833	0.882	0.797	0.637	0.811
	RMSE 5.35	3.34	3.21	3.88	4.85	6.05	4.25	3.89	3.71	3.50	3.52	3.98	5.81	5.92
mNDWI (2030, 2260)	R ² 0.736	0.789	0.831	0.828	0.792	0.728	0.688	0.692	0.799	0.898	0.892	0.824	0.750	0.837
	RMSE 4.09	3.31	2.61	3.31	4.25	5.17	3.70	3.43	3.15	2.45	2.71	2.87	5.00	5.25

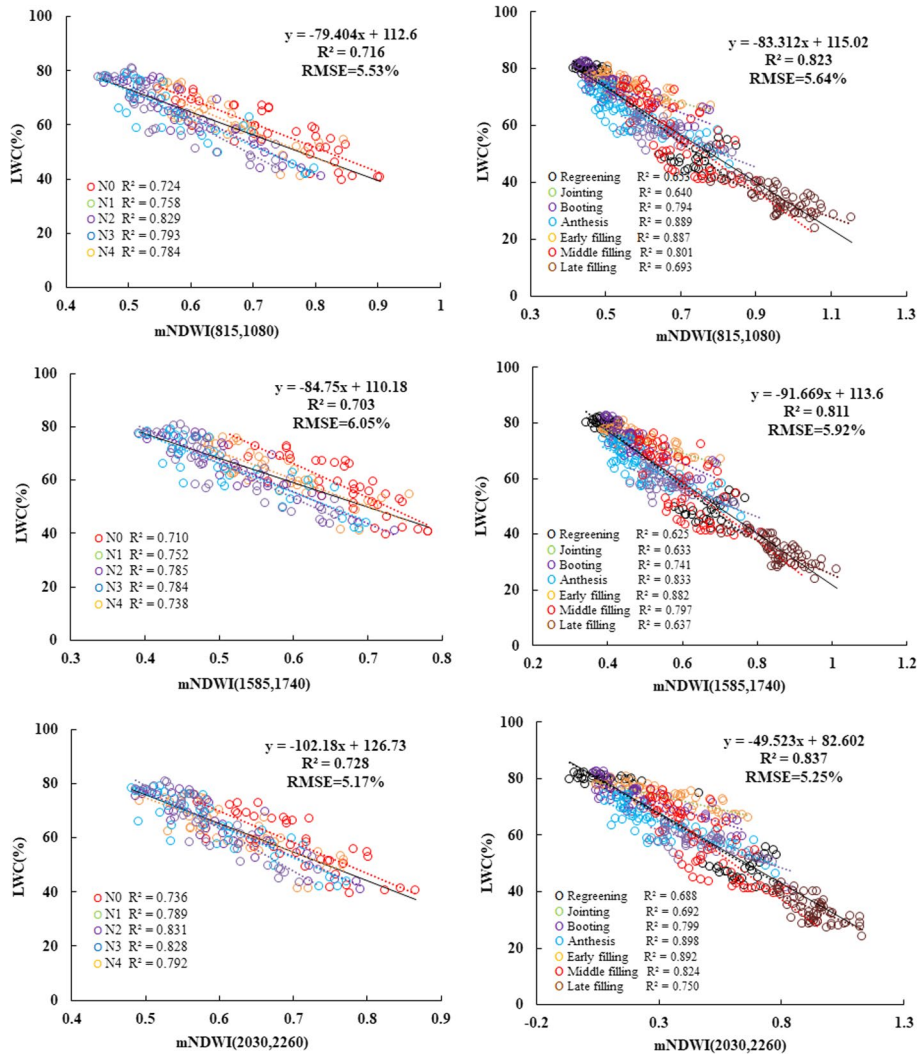


Fig. 8 Quantitative relationships between the LWC and the novel spectral indices mNDWI (815, 1080), mNDWI (1585, 1740), and mNDWI (2030, 2260) for five different nitrogen treatments and seven growth stages. (nregreening = 73, njointing = 60, nbooting = 76, nflowering = 94, ninitial-filling = 40, nmid-filling = 56, nlate-filling = 36, the number of each N treatment = 39)

further, the regression analysis between the conventional water vegetation index and the LWC showed clearly the phenomenon of “nitrogen treatment differentiation”. The distribution trend of the water concentration dataset for the different nitrogen treatments is inconsistent, and the slopes and intercepts of the regression equation are quite different, resulting in lower accuracy of the unified monitoring model under different nitrogen treatments. The conventional indices, NDII and NDSI (762, 1458, 2301), showed poor accuracy in monitoring LWC in the low nitrogen conditions (N0 and N1). This may be because when crops experience low-nitrogen stress, water absorption is restricted, resulting in lower vegetation

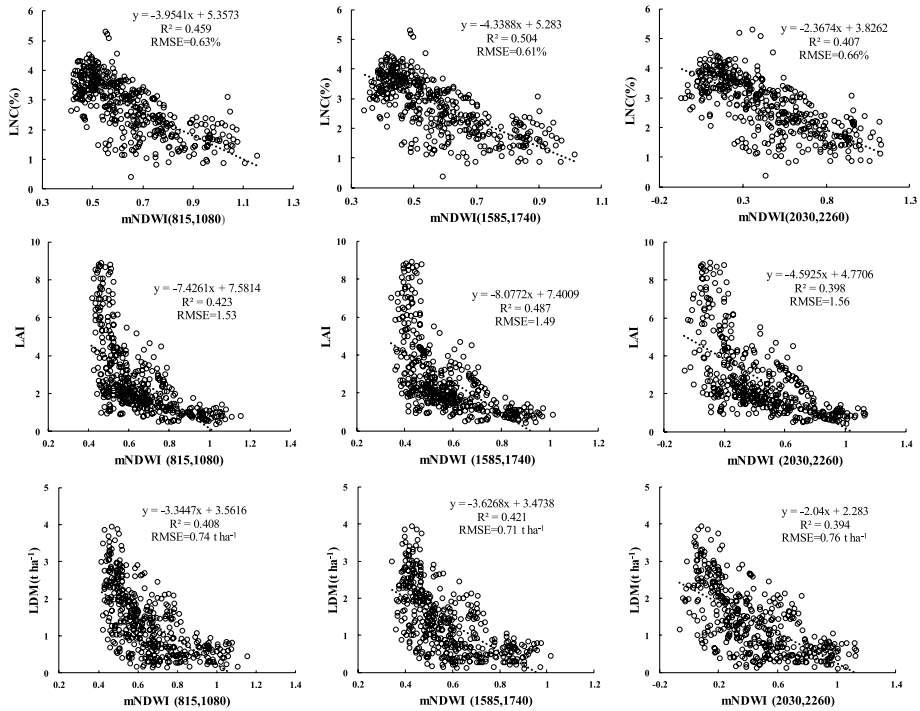


Fig. 9 Quantitative relationships between LNC, LAI, LDM and the novel spectral indices mNDWI (815, 1080), mNDWI (1585, 1740), and mNDWI (2030, 2260)

density, LAI and LDM, and the difference in spectral response between vegetation and the soil background gradually increases (Guo et al., 2019). When the amount of nitrogen applied exceeds the normal level, the monitoring accuracy of LWC is also low, which may be related to the saturation of leaf area, LDM and water indicators caused by excessive nitrogen application. The interaction of water and nitrogen in this study is the most common phenomenon encountered in monitoring wheat production. Hence, it is very important to decouple the interaction between water and nitrogen. Finding a way to reduce the influence of nitrogen while monitoring the water status, or to explore the vegetation index and monitoring model that is sensitive to water but insensitive to nitrogen, is of great significance for further improving the accuracy of water monitoring.

The effects of growth period on LWC estimation

The coverage of winter wheat changes constantly during each growth period, and different water and nitrogen treatments exacerbate the coverage difference. This study analyzed and compared the effects of various vegetation indices in monitoring LWC under different growth periods. For the same vegetation index, the regression model differs greatly during the growth period, and the monitoring accuracy tends to gradually increase and then decrease as the growth period advances. The main reason is that when wheat is in the regreening stage, the LAI, LDM and leaf angle distribution is low, so the plant structural characteristics are not obvious, leading to plant coverage that is low, and the vegetation

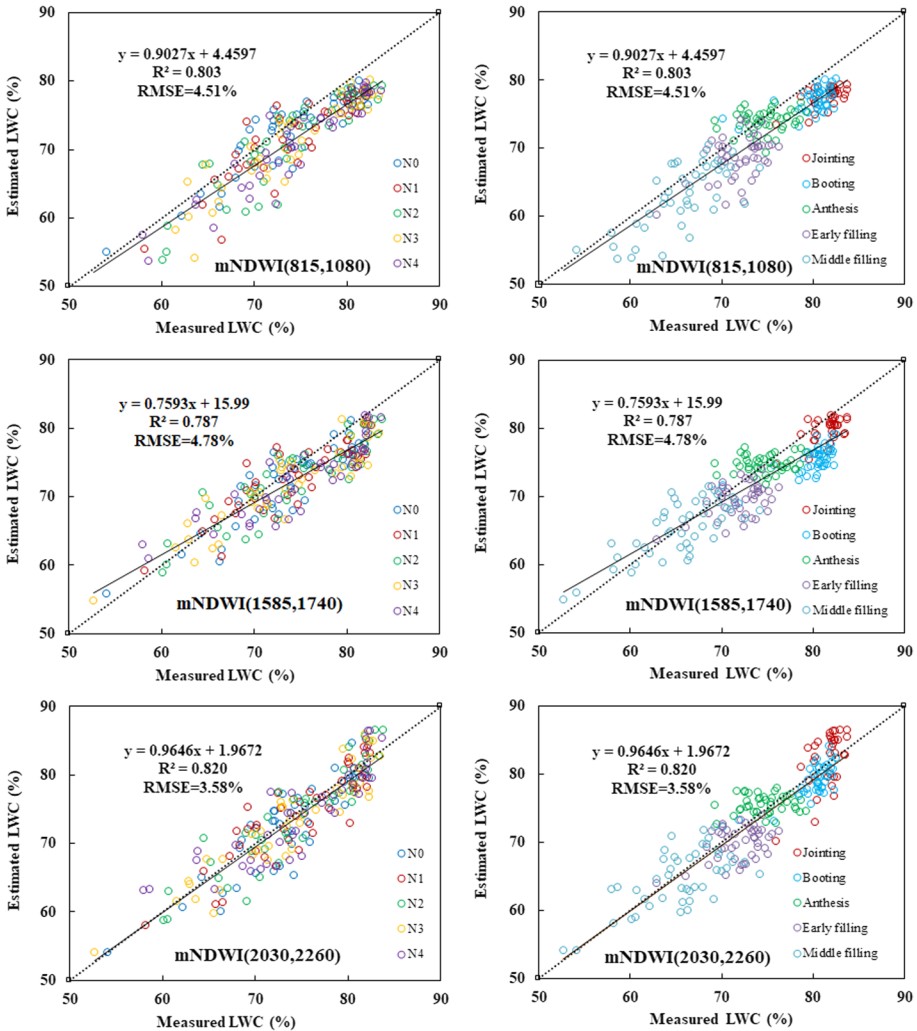


Fig. 10 Comparison of estimated and measured wheat LWC based on mNDWI (815, 1080), mNDWI (1585, 1740), and mNDWI (2030, 2260) for five different nitrogen treatments and five growth stages (n=215)

indices are greatly affected by soil background (Huang et al., 2005). Around anthesis, LAI reaches its maximum value and the leaves are fully extended, the crop coverage is relatively high, the observation field is dominated by wheat information, and the soil background has little effect on the reflectance of the wheat canopy (Zhao et al., 2013a). In the late filling stage, winter wheat transitions from vegetative growth to reproductive growth; nutrients in the leaves transfer to the wheat ears, the lower leaves become senescent and fall off, and the proportion of the soil background in the field of view increases once again (Zhang & Zhang, 2008). In addition, the water content of wheat stalks will also affect the mixed spectrum of the canopy, lignin accumulation in wheat stems showed a gradually increasing trend from the stem appeared. The bending resistance of the stem is higher during anthesis, and the storage material in the stem starts to break down and is transported into the

grain from the filling period, resulting in a substantial degree of decline in the mechanical hardness of the stems (Matos et al., 2013). The radiation at 970 nm cannot penetrate the increasingly hardened stalk tissue and therefore cannot convey information about the water contained within it (Woher et al., 2018). This further proves that the monitoring accuracy depends on the assessed crop's growth period.

In addition, the regression relationship between vegetation index and LWC shows obvious differentiation in the different growth periods, which makes it difficult to construct a unified LWC monitoring model for the entire growth period using a conventional water vegetation index, thus limiting its wide application in crop production. Previous studies have tried to solve the problem of growth period incompatibility when monitoring light energy and nitrogen utilization efficiency using the index difference method (Gitelson et al., 2017) and the introduced coefficient method (Zhang et al., 2018). In order to reduce the noise from plant nitrogen before and after anthesis, Yao et al. (2014) introduced the third band information indicating cellulose on the basis of the preferred spectral parameter NDSI (1429, 416). Although the three-band vegetation index partially alleviates the influence of the growth period when monitoring leaf EWT, the monitoring accuracy over the entire growth period still needs to be improved. Therefore, ways in which the other bands can be introduced on the basis of the water sensitive band and its combination, and reduce the growth period differentiation phenomenon from the conventional water index in monitoring crop water concentration, need further discussion.

The relationship between mNDWI and LWC

Screening water-sensitive bands is very important for constructing an LWC model. This study analyzed the relationship between the LWC and the spectral parameters of a random two-band normalized combination of 350–2500 nm, selected three large regions for monitoring LWC, i.e., the NIR/NIR band combination, the SWIR-1/SWIR-1 band combination, and the SWIR-2/SWIR-2 band combination. Water absorption is weak for the NIR region (900–1300 nm) due to the multiple scattering of NIR bands in the leaves, but the vegetation spectrum in this region is sensitive to LWC change, unless LAI reaches a high value (Lillesaeter, 1982). Previous studies also used NIR band combinations to establish vegetation indices for indicating water change; the normalized difference water index NDWI (860, 1240) based on the NDVI was built to estimate the canopy water content (Gao, 1996). The NIR (858) and SWIR (1240, 1640) bands in MODIS were used to construct the Short-wave Angle Normalized Index, which can effectively track water changes (Orueta et al., 2005). The leaf water absorption dominates the spectral reflectance in the 1350–2500 nm band. There are strong absorption characteristics of 1450 nm, 1940 nm and 2700 nm, and two main reflection peaks are near 1650 nm and 2200 nm. The 1550–1750 nm region was found to be best suited for remote sensing of plant canopy water status (Tucker, 1980). The first derivative index DR1653/DR1687 can monitor EWT and fuel moisture content (Yi et al., 2013). Sensitive bands at 2130 nm and 2301 nm were used for constructing the normalized multi-band drought index and NDSI (762, 1458, 2301) to estimate plant water changes (Wang & Qu, 2007; Yao et al., 2014). In this study, the optimized NDSI (815, 1080), NDSI (1585, 1740), and NDSI (2030, 2260) were selected based on the above three sensitive regions, but the selection of sensitive bands was carried out under different nitrogen levels, so the water sensitive bands may convey key nitrogen information. When monitoring the LWC using NDSI (815, 1080), NDSI (1585, 1740), and NDSI (2030, 2260), although the monitoring accuracy at different nitrogen levels and growth periods has been

improved, there are still the phenomena of “nitrogen treatment differentiation” and “growth period differentiation”. This screening method for sensitive bands further proves that it is necessary to reduce the influence of nitrogen on monitoring crop water status under different growth periods, to enhance the accuracy of water monitoring in actual production applications.

The physiological and ecological variables of the crop canopy are usually closely related. When monitoring a certain physiological variable, other closely related physiological and ecological factors often interfere with its monitoring effect. Previous studies have attempted to reduce the interaction influence between factors on remote sensing monitoring. In order to minimize the effect of water on nitrogen estimation, the water resistance vegetation index (WRNI) was constructed to improve the monitoring accuracy of LNC (Feng et al., 2016). The ratio of the transformed chlorophyll absorption reflectance index (TCARI) to soil canopy reflectivity (OSAVI) or extracting the characteristic chlorophyll bands can minimize the influence of vegetation structure variables and soil background on the monitoring of crop chlorophyll content (Cui et al., 2019; Haboudane et al., 2002). With the development of remote sensing research, the vegetation index has evolved from two-band to three-band or even multi-band, and the calculation framework of the spectral index has gradually diversified (Haboudane et al., 2002; Yao et al., 2014). For the optimized two-band normalized combination, especially for NDSI (1585, 1740) and NDSI (2030, 2260), the sensitive bands at 1740 nm and 2260 nm are the absorption peaks of protein, cellulose, and starch by stretch CH and rotation CH, CH₂, and stretch OH (Fourty et al., 1996), which can also be affected by nitrogen nutrition. Therefore, the decoupling of water and nitrogen cannot be ignored. Based on the sensitivity of RIDA to changes in LNC (Feng et al., 2014), RIDA may be used as a nitrogen indicator, which was introduced as a reduction coefficient into the water-sensitive two-band optimization combination (NDSI). In the formula, 815 nm, 1585 nm, and 2030 nm are the reference bands, and “1 + Ne” increases the role of the reference bands. The 1080 nm, 1740 nm, and 2260 nm bands are sensitive to water, especially 1740 nm and 2260 nm that are also affected by nitrogen-related compounds such as protein, cellulose, and starch. Thus, “1 – Ne” attenuates the nitrogen effect of 1080 nm, 1740 nm and 2260 nm, which decouples the effect of water and nitrogen on the same band. Compared with the conventional vegetation index and the sensitive band combinations, the newly derived water index, mNDWI, weakens the influence of nitrogen on water monitoring under different growth periods. This effectively alleviates the “nitrogen treatment differentiation” and “growth period differentiation” phenomena, and greatly enhances the practicality of mNDWI in actual production.

In the practice of wheat production, the soil fertility or the nitrogen applied may be different, the precise identification ability of the crop growth period is poor, which limits the application of conventional moisture vegetation indices. The new water index established in this study can provide method reference and technical support for accurately evaluating crop water concentration under different nitrogen fertilizer rates and growth period conditions. The water estimation model constructed in this experiment using many years, multiple points, and multiple varieties has good accuracy and applicability. Nevertheless, the vegetation index and the monitoring model still need to be verified on more regions and on other spatial scales, especially the optimal bandwidths of mNDWI for use with the UAV platform (including other middle-infrared bands), so as to provide robust technical support for large-scale water monitoring and the precise irrigation of wheat.

Conclusions

Hyperspectral reflection data can quickly and non-destructively diagnose crop water stress status, which is important for guiding winter wheat growth monitoring and variable irrigation decision-making. Different nitrogen treatments and irrigation systems significantly affect the temporal and spatial characteristics of canopy reflectance, which in turn leads to the phenomenon of “nitrogen treatment differentiation” and “growth period differentiation” for the conventional vegetation water index NDSI (762, 1458, 2301) and NDII monitoring models. Through the normalized optimization combination analysis of any two bands in the 350–2500 nm range, there are five water-sensitive combination regions, and the bands with good correlation to LWC are mainly concentrated in the 770–1120 nm, 1565–1780 nm, and 2020–2300 nm ranges. On the basis of the optimized normalized band combination, the nitrogen factor RIDA was introduced to construct a modified multi-band water index, mNDWI. Compared with the conventional water index NDSI (762, 1458, 2301), the monitoring accuracy of mNDWI, especially mNDWI (815, 1080) and mNDWI (2030, 2260) under different nitrogen treatments and growth periods increased by more than 18.6%, effectively reducing the impact of nitrogen status on the LWC monitoring model and realizing the unified modeling and accurate inversion of LWC for the entire growth period. This indicates that the application of hyperspectral reflection data can better convey the LWC status of the winter wheat crop under its different growth conditions, which is important for the real-time diagnosis of plant moisture to guide precision field irrigation applications.

Acknowledgements This work was supported by grants from the Key Technologies Research and Development Program of Henan Province, China (Grant No. 212102110041), the National Natural Science Foundation of China (Grant No. 32271991); and the Research Start-up Fund to Young Talents of Henan Agricultural University (Grant No. 30601648).

Author contributions Conceptualization: LH and WF; Methodology: LH; Formal analysis and investigation: M-RL, S-HZ, and H-WG; Writing-original draft preparation: LH; Writing-review and editing: WF and C-YW; Funding acquisition: T-CG.

Data availability The data that support the findings of this study are available from the corresponding author upon reasonable request.

Declarations

Conflict of interest The authors declare that they have no conflicts of interest.

References

- Bandyopadhyay, K. K., Pradhan, S., Sahoo, R. N., Singh, R., Gupta, V. K., Joshi, D. K., & Sutradhar, A. K. (2014). Characterization of water stress and prediction of yield of wheat using spectral indices under varied water and nitrogen management practices. *Agricultural Water Management*, *146*, 115–123. <https://doi.org/10.1016/j.agwat.2014.07.017>
- Berger, K., Verrelst, J., Feret, J. B., Wang, Z. H., Woche, M., Strathmann, M., Danner, M., Mauser, W., & Hank, T. (2020). Crop nitrogen monitoring: Recent progress and principal developments in the context of imaging spectroscopy missions. *Remote Sensing of Environment*. <https://doi.org/10.1016/j.rse.2020.111758>

- Ceccato, P., Flasse, S., Tarantola, S., Jacquemoud, S., & Grégoire, J. (2001). Detecting vegetation leaf water content using reflectance in the optical domain. *Remote Sensing of Environment*, *77*, 22–33. [https://doi.org/10.1016/S0034-4257\(01\)00191-2](https://doi.org/10.1016/S0034-4257(01)00191-2)
- Chen, D. Y., Huang, J. F., & Jackson, T. J. (2005). Vegetation water content estimation for corn and soybeans using spectral indices derived from MODIS near- and short-wave infrared bands. *Remote Sensing of Environment*, *98*, 225–236. <https://doi.org/10.1016/j.rse.2005.07.008>
- Cheng, T., Rivard, B., Sánchez-Azofeifa, A. G., Féret, J. B., Jacquemoud, S., & Ustin, S. L. (2012). Predicting leaf gravimetric water content from foliar reflectance across a range of plant species using continuous wavelet analysis. *Journal of Plant Physiology*, *169*, 1134–1142. <https://doi.org/10.1016/j.jplph.2012.04.006>
- Cho, M. A., & Skidmore, A. K. (2006). A new technique for extracting the red edge position from hyperspectral data: The linear extrapolation method. *Remote Sensing of Environment*, *101*, 181–193. <https://doi.org/10.1016/j.rse.2005.12.011>
- Cooper, P. J. M., Gregory, P. J., Keatinge, J. D. H., & Brown, S. C. (1987). Effects of fertilizer, variety and location on barley production under rainfed conditions in northern Syria 2. Soil water dynamics and crop water use. *Field Crops Research*, *16*, 67–84. [https://doi.org/10.1016/0378-4290\(87\)90054-2](https://doi.org/10.1016/0378-4290(87)90054-2)
- Cui, B., Zhao, Q. J., Huang, W. J., Song, X. Y., Ye, H. C., & Zhou, X. F. (2019). A new integrated vegetation index for the estimation of winter wheat leaf chlorophyll content. *Remote Sensing*, *11*, 974. <https://doi.org/10.3390/rs11080974>
- Danson, F. M., Steven, M. D., Malthus, T. J., & Clark, J. A. (1992). High-spectral resolution data for determining leaf water content. *International Journal of Remote Sensing*, *13*, 461–470. <https://doi.org/10.7522/j.issn.1000-694X.2013.00403>
- Das, B., Sahoo, R. N., Pargal, S., Krishna, G., Vcerma, R., Viswanathan, C., Sehgal, V. K., & Gupta, V. K. (2017). Comparison of different uni- and multi-variate techniques for monitoring leaf water status as an indicator of water-deficit stress in wheat through spectroscopy. *Biosystems Engineering*, *160*, 69–83. <https://doi.org/10.1016/j.biosystemseng.2017.05.007>
- Elsayed, S., Elhoweity, M., Ibrahim, H. H., Dewir, Y. H., Migdadi, H. M., & Schmidhalter, U. (2017). Thermal imaging and passive reflectance sensing to estimate the water status and grain yield of wheat under different irrigation regimes. *Agricultural Water Management*, *189*, 98–110. <https://doi.org/10.1016/j.agwat.2017.05.001>
- Feng, W., Guo, B. B., Wang, Z. J., He, L., Song, X., Wang, Y. H., & Guo, T. C. (2014). Measuring leaf nitrogen concentration in winter wheat using double-peak spectral reflection remote sensing data. *Field Crops Research*, *159*, 43–52. <https://doi.org/10.1016/j.fcr.2014.01.010>
- Feng, W., Zhang, H. Y., Zhang, Y. S., Qi, S. L., Heng, Y. R., Guo, B. B., Ma, D. Y., & Guo, T. C. (2016). Remote detection of canopy leaf nitrogen concentration in winter wheat by using water resistance vegetation indices from in-situ hyperspectral data. *Field Crops Research*, *198*, 238–246. <https://doi.org/10.1016/j.fcr.2016.08.023>
- Fitzgerald, G. J., Rodriguez, D., Christensen, L. K., Belford, K., Sadras, V. O., & Clarke, T. R. (2006). Spectral and thermal sensing for nitrogen and water status in rainfed and irrigated wheat environments. *Precision Agriculture*, *7*, 233–248. <https://doi.org/10.1007/s11119-006-9011-z>
- Fourty, T. H., Baret, F., Jacquemoud, S., Schmuck, G., & Verdebout, J. (1996). Leaf optical properties with explicit description of its biochemical composition: Direct and inverse problems. *Remote Sensing of Environment*, *56*, 104–117.
- Gao, B. C. (1996). NDWI—A normalized difference water index for remote sensing of vegetation liquid water from space. *Remote Sensing of Environment*, *58*, 257–266. <https://doi.org/10.1117/12.210877>
- Gitelson, A. A., Gamon, J. A., & Solovchenko, A. (2017). Multiple drivers of seasonal change in PRI: Implications for photosynthesis 2. *Stand Level. Remote Sensing of Environment*, *190*, 198–206. <https://doi.org/10.1016/j.rse.2016.12.015>
- Gizaw, S. A., Campbell, K. G., & Carter, A. H. (2016). Evaluation of agronomic traits and spectral reflectance in Pacific Northwest winter wheat under rain-fed and irrigated conditions. *Field Crops Research*, *196*, 168–179. <https://doi.org/10.1016/j.fcr.2016.06.018>
- Gong, P., Pu, R. L., & Heald, R. C. (2002). Analysis of in situ hyperspectral data for nutrient estimation of giant sequoia. *International Journal of Remote Sensing*, *23*, 1827–1850. <https://doi.org/10.1080/01431160110075622>
- Guo, J., Gao, Y., Li, S., Pema, R., Wang, Y., Zhang, Y., & Liu, R. (2019). Estimation model of leaf water content of winter wheat based on multi-angle hyperspectral remote sensing. *Journal of Anhui Agricultural University*, *46*, 124–132. <https://doi.org/10.3389/fpls.2021.614417>
- Haboudane, D., Miller, J. R., Tremblay, N., Zarco-Tejada, P. J., & Dextraze, L. (2002). Integrated narrow-band vegetation indices for prediction of crop chlorophyll content for application to precision


- agriculture. *Remote Sensing of Environment*, 81, 416–426. [https://doi.org/10.1016/S0034-4257\(02\)00018-4](https://doi.org/10.1016/S0034-4257(02)00018-4)
- Hendawy, S. E. E., Suhaibani, N. A. A., Elsayed, S., Hassan, W. M., Dewir, Y. H., Refay, Y., & Abdella, K. A. (2019). Potential of the existing and novel spectral reflectance indices for estimating the leaf water status and grain yield of spring wheat exposed to different irrigation rates. *Agricultural Water Management*, 217, 356–373. <https://doi.org/10.1016/j.agwat.2019.03.006>
- Huang, W. J., Wang, J. H., Liu, L. Y., Wang, J. D., Tan, C. W., Li, C. J., et al. (2005). Remote sensing identification of plant structural types based on multi-temporal and bidirectional canopy spectrum. *Transactions of the Chinese Society of Agricultural Engineering*, 21, 82–86. (in Chinese with English abstract). [https://doi.org/10.1016/0090-4295\(80\)90421-5](https://doi.org/10.1016/0090-4295(80)90421-5).
- Huete, A., Didan, K., Miura, T., Rodriguez, E. P., Gao, X., & Ferreira, L. G. (2002). Overview of the radiometric and biophysical performance of the MODIS vegetation indices. *Remote Sensing of Environment*, 83, 195–213. [https://doi.org/10.1016/S0034-4257\(02\)00096-2](https://doi.org/10.1016/S0034-4257(02)00096-2)
- Klem, K., Zahora, J., Zemek, F., Trunda, P., Tuma, I., Novotna, K., Hodaňová, P., Rapantová, B., Hanuš, J., Vavříková, J., & Holub, P. (2018). Interactive effects of water deficit and nitrogen nutrition on winter wheat, remote sensing methods for their detection. *Agricultural Water Management*, 210, 171–184. <https://doi.org/10.1016/j.agwat.2018.08.004>
- Kong, W. P., Huang, W. J., Ma, L. L., Tang, L. L., Li, C. R., Zhou, X. F., & Casa, R. (2021). Estimating vertical distribution of leaf water content within wheat canopies after head emergence. *Remote Sensing*, 13, 4125. <https://doi.org/10.3390/rs13204125>
- Krishna, G., Sahoo, R. N., Singh, P., Bajpai, V., Patra, H., Kumar, S., Dandapani, R., Gupta, V. K., Viswanathan, C., Ahmad, T., & Sahoo, P. M. (2019). Comparison of various modeling approaches for water deficit stress monitoring in rice crop through hyperspectral remote sensing. *Agricultural Water Management*, 213, 231–244. <https://doi.org/10.1016/j.agwat.2018.08.029>
- Lillesaeter, O. (1982). Spectral reflectance of partly transmitting leaves: Laboratory measurements and mathematical modeling. *Remote Sensing of Environment*, 12, 247–254.
- Liu, L. Y., Wang, J. H., Huang, W. J., Zhao, C. J., Zhang, B., & Tong, Q. X. (2004). Estimating winter wheat plant water content using red edge parameters. *International Journal of Remote Sensing*, 17, 3331–3342. <https://doi.org/10.1080/01431160310001654365>
- Matos, D. A., Whitney, L. P., Harrington, M. J., & Hazen, S. P. (2013). Cell walls and the developmental anatomy of the *Brachypodium distachyon* stem internode. *PLoS ONE*. <https://doi.org/10.1371/journal.pone.0080640>
- Orueta, A. P., Khanna, S., Litago, J., Whiting, M. L., & Ustin, S. (2005). Assessment of NDVI and NDWI spectral indices using MODIS time series analysis and development of a new spectral index based on MODIS shortwave infrared bands. The 1st International Conference of Remote Sensing and Geoinformation Processing, Trier, Germany: Universitat Trier publishers.
- Peng, Y., & Gitelson, A. A. (2011). Application of chlorophyll-related vegetation indices for remote estimation of maize productivity. *Agricultural and Forest Meteorology*, 151, 1267–1276. <https://doi.org/10.1016/j.agrformet.2011.05.005>
- Peñuelas, J., Filella, I., Biel, C., Serrano, L., & Save, R. (1993). The reflectance at the 950–970 nm region as an indicator of plant water status. *International Journal of Remote Sensing*, 14, 1887–1905. <https://doi.org/10.1080/01431169308954010>
- Peñuelas, J., & Inoue, Y. (1999). Reflectance indices indicative of changes in water and pigment contents of peanut and wheat leaves. *Photosynthetica*, 36, 355–360. <https://doi.org/10.1023/A:1007033503276>
- Peñuelas, J., Piñol, J., Ogaya, R., & Filella, I. (1997). Estimation of plant water concentration by the reflectance water index WI (R900/R970). *International Journal of Remote Sensing*, 18, 2869–2875. <https://doi.org/10.1080/014311697217396>
- Pu, R. L., & Gong, P. (2000). *Hyperspectral remote sensing and its applications*. Higher Education Press.
- Quintero, J. M., Fournier, J. M., & Benlloch, M. (1999). Water transport in sunflower root systems: Effects of ABA, Ca²⁺ status and HgCl₂. *Journal of Experimental Botany*, 50, 1607–1612. <https://doi.org/10.1093/jxb/50.339.1607>
- Strachan, I. B., Pattey, E., & Boisvert, J. B. (2002). Impact of nitrogen and environmental conditions on corn as detected by hyperspectral reflectance. *Remote Sensing of Environment*, 80, 213–224. [https://doi.org/10.1016/S0034-4257\(01\)00299-1](https://doi.org/10.1016/S0034-4257(01)00299-1)
- Thomas, J. R., Namken, L. N., Oerther, G. F., & Brown, R. G. (1971). Estimating leaf water content by reflectance measurements. *Agronomy Journal*, 63, 845–847.
- Tucker, C. J. (1980). Remote sensing of leaf water content in the near-infrared. *Remote Sensing of Environment*, 10, 23–32.
- Wang, C., Liu, W., Li, Q., Ma, D. Y., Lu, H., Feng, W., Zhu, Y., & Guo, T. (2014). Effects of different irrigation and nitrogen regimes on root growth and its correlation with above-ground plant parts in

- high-yielding wheat under field conditions. *Field Crops Research*, 165, 138–149. <https://doi.org/10.1016/j.fcr.2014.04.011>
- Wang, H. L., Chen, A. F., Wang, Q. F., & He, B. (2015). Drought dynamics and impacts on vegetation in China from 1982 to 2011. *Ecological Engineering*, 75, 303–307. <https://doi.org/10.1016/j.ecoleng.2014.11.063>
- Wang, L. L., & Qu, J. (2007). NMDI: A normalized multi-band drought index for monitoring soil and vegetation moisture with satellite remote sensing. *Geophysical Research Letters*, 34, L20405. <https://doi.org/10.1029/2007GL031021>
- Wang, Y., Li, G., Zhang, L., & Fan, J. (2011). Retrieval of leaf water content of winter wheat from canopy spectral reflectance data using a position index (λ_{\min}) derived from the 1200 nm absorption band. *Remote Sensing Letters*, 2, 31–40. <https://doi.org/10.1080/01431161.2010.490797>
- Woche, M., Berger, K., Danner, M., Mauser, W., & Hank, T. (2018). Physically-Based retrieval of canopy equivalent water thickness using hyperspectral data. *Remote Sensing*, 10, 1924. <https://doi.org/10.3390/rs10121924>
- Yao, X., Jia, W. Q., Si, H., Guo, Z., Tian, Y., Liu, X., Cao, W., & Zhu, Y. (2014). Exploring novel bands and key index for evaluating leaf equivalent water thickness in wheat using hyperspectra influenced by nitrogen. *PLoS ONE*. <https://doi.org/10.1371/journal.pone.0096352>
- Yi, Q. X., Bao, A. M., Wang, Q., & Zhao, J. (2013). Estimation of leaf water content in cotton by means of hyperspectral indices. *Computers and Electronics in Agriculture*, 90, 144–151. <https://doi.org/10.1016/j.compag.2012.09.011>
- Yilmaz, M. T., Hunt, E. R., Jr., & Jackson, T. J. (2008). Remote sensing of vegetation water content from equivalent water thickness using satellite imagery. *Remote Sensing of Environment*, 112, 2514–2522. <https://doi.org/10.1016/j.rse.2007.11.014>
- Yu, G. R., Miwa, T., Nakayama, K., Matsuoka, N., & Kon, H. A. (2000). A proposal for universal formulas for estimating leaf water status of herbaceous and woody plants based on spectral reflectance properties. *Plant and Soil*, 227, 47–58.
- Zarco-Tejada, P. J., Miller, J. R., Mohammed, G. H., Noland, T. L., & Sampson, P. H. (2001). Scaling-up and model inversion methods with narrow-band optical indices for chlorophyll content estimation in closed forest canopies with hyperspectral data. *IEEE Transactions on Geoscience Remote Sensing*, 39, 1491–1507.
- Zarco-Tejada, P. J., Rueda, C. A., & Ustin, S. L. (2003). Water content estimation in vegetation with MODIS reflectance data and model inversion methods. *Remote Sensing of Environment*, 85, 109–124. [https://doi.org/10.1016/S0034-4257\(02\)00197-9](https://doi.org/10.1016/S0034-4257(02)00197-9)
- Zhang, H. Y., Ren, X. X., Zhou, Y., Wu, Y. P., He, L., Heng, Y. R., Feng, W., & Wang, C. Y. (2018). Remotely assessing photosynthetic nitrogen use efficiency with in situ hyperspectral remote sensing in winter wheat. *European Journal of Agronomy*, 101, 90–100. <https://doi.org/10.1016/j.eja.2018.08.010>
- Zhang, J. H., & Zhang, J. B. (2008). Response of winter wheat spectral reflectance to leaf chlorophyll, total nitrogen of above ground. *Chinese Journal of Soil Science*, 39, 586–592. <https://doi.org/10.1163/156939308783122788>
- Zhao, J., Huang, W. J., Zhang, Y. H., & Jing, Y. S. (2013a). Inversion of leaf area index during different growth stages in winter wheat. *Spectroscopy and Spectral Analysis*, 33, 2546–2552.
- Zhao, K., Valle, D., Popescu, S., Zhang, X., & Mallick, B. (2013b). Hyperspectral remote sensing of plant biochemistry using Bayesian model averaging with variable and band selection. *Remote Sensing of Environment*, 132, 102–119. <https://doi.org/10.1016/j.rse.2012.12.026>

Publisher's Note Springer Nature remains neutral with regard to jurisdictional claims in published maps and institutional affiliations.

Springer Nature or its licensor (e.g. a society or other partner) holds exclusive rights to this article under a publishing agreement with the author(s) or other rightsholder(s); author self-archiving of the accepted manuscript version of this article is solely governed by the terms of such publishing agreement and applicable law.

Authors and Affiliations

Li He^{1,2,3} · **Meng-Ran Liu**¹ · **Shao-Hua Zhang**¹ · **Han-Wen Guan**¹ · **Chen-Yang Wang**^{1,3} · **Wei Feng**^{1,2,3}  · **Tian-Cai Guo**^{1,3}

- ¹ Present Address: College of Agronomy/State Key Laboratory of Wheat and Maize Crop Science, Henan Agricultural University, #15 Longzihu College District, Zhengzhou, Henan 450046, People's Republic of China
- ² CIMMYT-China Joint Center of Wheat and Maize Improvement, #15 Longzihu College District, Zhengzhou, Henan 450046, People's Republic of China
- ³ Henan Technology Innovation Centre of Wheat, #15 Longzihu College District, Zhengzhou, Henan 450046, People's Republic of China